NUMERICAL SOLUTION OF A CLASS OF ADVECTION-REACTION-DIFFUSION SYSTEM

by

Li CAO [a,c] ***and Zhanxin MA*** [b*]

[a] School of Mathematics Science, Inner Mongolia University, Hohhot, Inner Mongolia, China
[b] School of Economics and Management, Inner Mongolia University, Hohhot, Inner Mongolia, China
[c] College of Computer and Information, Inner Mongolia Medical University, Hohhot, Inner Mongolia, China

Original scientific paper
https://doi.org/10.2298/TSCI180803217C

In this article, the barycentric interpolation collocation methods is proposed for solving a class of non-linear advection-reaction-diffusion system. Compared with other methods, the numerical experiment shows the barycentric interpolation collocation method is a high precision method to solve the advection- reaction-diffusion system.

Key words: *non-linear advection-reaction-diffusion problems, numerical experiment, barycentric interpolation collocation method*

Introduction

The treatise is devoted to the numerical solution of a class of non-linear advection-reaction-diffusion system. In this paper, the general expression of such system:

$$\begin{cases} \dfrac{\partial u}{\partial t} = d_1 \dfrac{\partial^2 u}{\partial x^2} + a_1 \dfrac{\partial u}{\partial x} + h_1(u,v), \\ \dfrac{\partial v}{\partial t} = d_2 \dfrac{\partial^2 u}{\partial x^2} + a_2 \dfrac{\partial u}{\partial x} + h_2(u,v), \end{cases} \quad a \le x \le b, \quad 0 \le t \le T \tag{1}$$

with the following initial boundary conditions:

$$\begin{aligned} & u(x,0) = f_0(x), \quad v(x,0) = g_0(x), \quad a \le x \le b, \quad 0 \le t \le T \\ & u(a,t) = f_1(t), \quad u(b,t) = f_2(t), \quad 0 \le t \le T \\ & v(a,t) = g_1(t), \quad v(b,t) = g_2(t) \end{aligned} \tag{2}$$

where a_1 and a_2 represent the of the transport medium, such as water or air, and both $d_1 > 0$ and $d_1 > 0$ are diffusion coefficients, which include the parametrizations of the turbulence.

The advection-reaction-diffusion system has wide applications in thermal science, chemical and mechanics. There are some valuable efforts that focus on finding the analytical and numerical methods for solving the advection-reaction-diffusion system. These methods include B-spline method [1, 2] the variational iteration method [3], homotopy perturbation method [4], integral transform [5], and so on [6, 7]. The barycentric interpolation collocation method [8-13] is a high precision method. In this paper, we mainly employ the barycentric Lagrange barycentric interpolation collocation method to solve the systems (1).

[*] Corresponding author, e-mail: em_mazhanxin@imu.edu.cn

Description of the numerical method

We give two initial functions u_0, v_0, and construct following linear iterative format:

$$\begin{cases} \dfrac{\partial u_n}{\partial t} = d_1 \dfrac{\partial^2 u_n}{\partial x^2} + a_1 \dfrac{\partial u_n}{\partial x} + h_1\left(u_{n-1}, v_{n-1}\right), \\ \dfrac{\partial v_n}{\partial t} = d_2 \dfrac{\partial^2 v_n}{\partial x^2} + a_2 \dfrac{\partial v_n}{\partial x} + h_2\left(u_{n-1}, v_{n-1}\right) \end{cases} \quad n = 1, 2, 3, \cdots. \tag{3}$$

Next, we use barycentric interpolation collocation method to solve eq. (3).

Let $a \le x_1 < x_2 < ... < x_M \le b$, $0 \le t_1 < t_2 < ... < t_N \le T$, respectively, These nodes can generate 2-D nodes on the rectangular are a $\Omega = [a, b] \times [0, T]$, as:

$$\{(x_i, t_j), i = 1, 2, ..., M; j = 1, 2, ...N\}$$

The barycenter interpolation form of function $u(x, t)$ can be expressed:

$$u(x,t) = \sum_{i=1}^{M} \sum_{j=1}^{N} \xi_i(x) \eta_j(t) u(x_i, t_j) \tag{4}$$

where

$$\xi_i(x) = \frac{\prod\limits_{k=1, k\ne i}^{M} (x - x_k)}{\prod\limits_{k=1, k\ne i}^{M} (x_i - x_k)}, i = 1, 2, \cdots, M, \quad \eta_j(t) = \frac{\prod\limits_{k=1, k\ne j}^{N} (t - t_k)}{\prod\limits_{k=1, k\ne j}^{N} (t_j - t_k)}, j = 1, 2, \cdots, N$$

According to eq. (4), the partial derivative of $l + k$ order of function $u(x, t)$ at the nodes (x_p, t_q) can be written:

$$u^{(l,k)}(x_p, t_q) := \frac{\partial^{l+k} u(x_p, t_q)}{\partial x^l \partial t^k} = \sum_{i=1}^{M} \sum_{j=1}^{N} \xi_i^{(l)}(x_p) \eta_j^{(k)}(t_q) u(x_i, t_j), \quad p = 1, 2, \cdots M; q = 1, 2, \cdots N \tag{5}$$

The function values of the eq. (4) and the eq. (5) at the node form column vectors u, $u^{(l,k)}$ and they are:

$$u = [u_1, u_2, \cdots, u_{M\times N}]^T, u^{(l,k)} = [u_1^{(l,k)}, u_2^{(l,k)}, \cdots, u_{M\times N}^{(l,k)}]^T$$
$$u_p = u(X_p, T_q), u_p^{(l,k)} = u^{(l,k)}(X_p, T_p), \quad p = 1, 2, \cdots, M \times N$$

Therefore, the eq. (5) can be expressed in the following matrix form:

$$u^{(l,k)} = D^{(l,k)} u \tag{6}$$

in the eq. (6), $D^{(l,k)} = C^{(l)} \otimes D^{(k)}$ is the Kronecker product of matrix $C^{(l)}$ and $D^{(k)}$, and it also called $l + k$ order partial differential matrix at nodes$\{(x_i, t_j), i = 1, 2, ..., M, j = 1, 2, ..., N\}$, $C^{(l)}$ and $D^{(k)}$ are l, k order differential matrices formed by barycenter interpolation at node interval $[a, b]$ and interval $[0, T]$, respectively. Let:

$$D^{(0)} = I_M, \quad D^{(0)} = I_N \tag{7}$$

where I_M and I_N are M order unit matrix and N order unit matrix, respectively .

So, the discrete form of the eq. (3) can be written:

$$\begin{cases} D^{(0,1)} u_n - d_1 D^{(2,0)} u_n - a_1 D^{(1,0)} u_n = diag[h_1(u_{n-1}, v_{n-1})] \\ D^{(0,1)} v_n - d_2 D^{(2,0)} v_n - a_2 D^{(1,0)} v_n = diag[h_2(u_{n-1}, v_{n-1})] \end{cases} \tag{8}$$

So, eq. (8) can be written in following partitioned matrix form:

$$\begin{bmatrix} D^{(0,1)} - d_1 D^{(2,0)} & 0 \\ 0 & D^{(0,1)} - d_2 D^{(2,0)} \end{bmatrix} \begin{bmatrix} u_n \\ v_n \end{bmatrix} = \begin{bmatrix} diag[h_1(u_{n-1}, v_{n-1})] \\ diag[h_2(u_{n-1}, v_{n-1})] \end{bmatrix} \tag{9}$$

In this paper, we use displacement method to impose the initial boundary conditions. The detailed procedure see [8-10]. In calculation, we choose the chebyshev nodes. In the following numerical experiments, we set a calculation accuracy $\varepsilon = 10^{-15}$, if $|u_n(x, t) - u_{n-1}(x, t)| < \varepsilon$ then the iteration stops.

Numerical experiments

Experiment 1. We consider the following dvection-reaction-diffusion problem [6]:

$$\begin{cases} \dfrac{\partial u}{\partial t} = d_1 \dfrac{\partial^2 u}{\partial x^2} + a_1 \dfrac{\partial u}{\partial x} + (a_1 - d_1)t + d_1 u - a_1 v + (u - v)^2 + \sin(2x) \\ \dfrac{\partial v}{\partial t} = d_2 \dfrac{\partial^2 v}{\partial x^2} + a_2 \dfrac{\partial v}{\partial x} + (a_2 - d_2)t + a_2 u + d_2 v + u^2 + v^2 - 2t(u + v) + 2t^2 \end{cases} \tag{10}$$

here the initial and boundary conditions are:

$$u(x, 0) = \sin x, \quad v(x, 0) = \cos x, \quad x \in [0, 4\pi] \tag{11}$$

$$u(0, t) = u(4\pi, t) = t, \quad v(0, t) = v(4\pi, t) = t + 1, \quad t \in [0, 1] \tag{12}$$

The exact solution of the equations is given by $u(x, t) = t + \sin(x)$, $v(x, t) = t + \cos(x)$. We select $d_1 = 0.5$, $d_2 = 0.1$, $a_1 = 0.5$, $a_2 = 0.1$. Numerical results are showed in figs. 1-6 and tabs. 1-3. In tab. 1, comparing the calculation time and error between the present method and other methods [6] under different nodes, we can find that the present method has the least calculation time and the least error. Tables 2 and 3 show the absolute errors in different nodes. As can be seen from the tabs. 2 and 3, with the increase of nodes, the absolute error is also decreasing. Figures 1-6 are numerical solutions and absolute errors in different nodes. It can be seen that the absolute error is very small. Obviously, our method is very suitable for solving such problems.

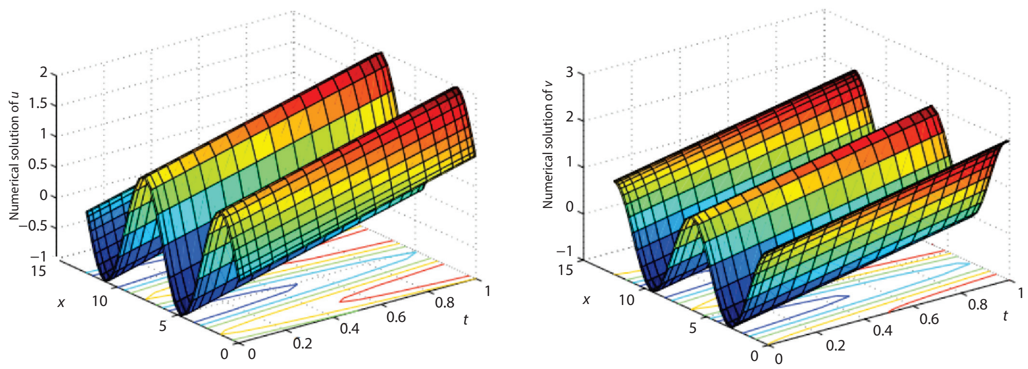

Figure 1. Numerical solutions obtained by the present method for *Experiment 1* with $M = 40$, $N = 20$

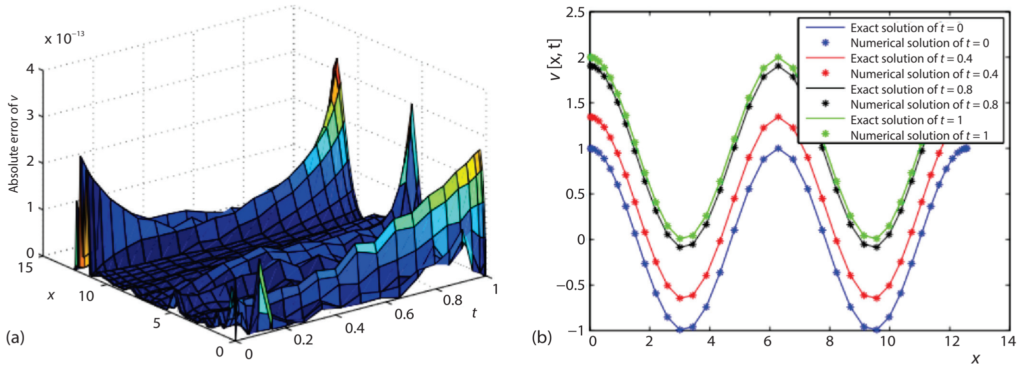

Figure 2. (a) Absolute errors of v and (b) comparisons between numerical and exact solutions of v for *Experiment 1* with M = 40, N = 20

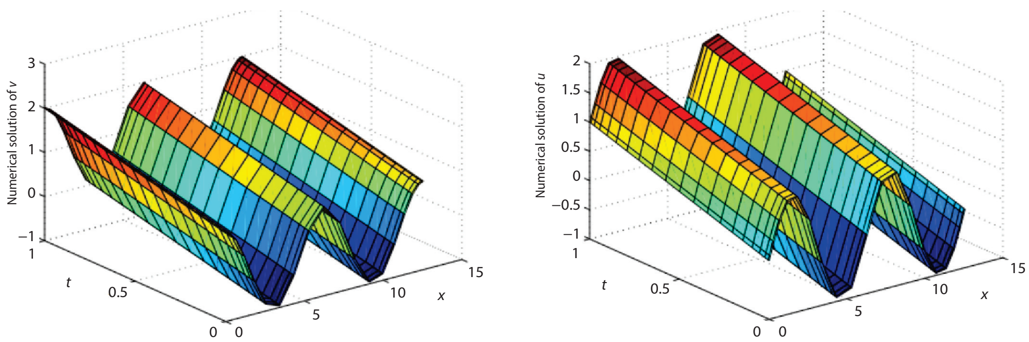

Figure 3. Numerical solutions for *Experiment 1* with M = 20, N = 20

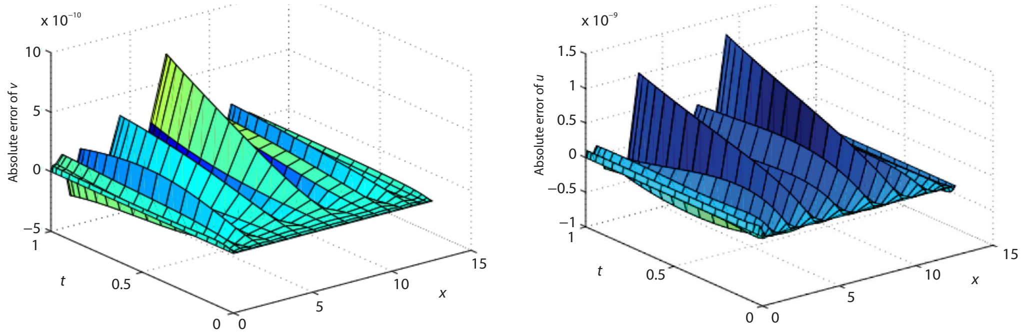

Figure 4. Absolute errors for *Experiment 1* with M = 20, N = 20

Table 1. Comparison of L_∞ error norm for *Experiment 1*

Method	M	CPU time	L_∞ error
Present method	20	6.9844	1.3107-7
IMEX-TF [6]	20	114.551534	0.000006
IMEX-class [6]	20	7.254047	0.103574
Present method	40	34.1141	2.5390-12
IMEX-class [6]	40	78.499703	0.025453
IMEX-class [6]	80	29.452989	0.006355
IMEX-class [6]	160	132.944052	0.001592
IMEX-class [6]	320	1627.527233	0.000398
IMEX-class [6]	640	14774.495908	0.000099

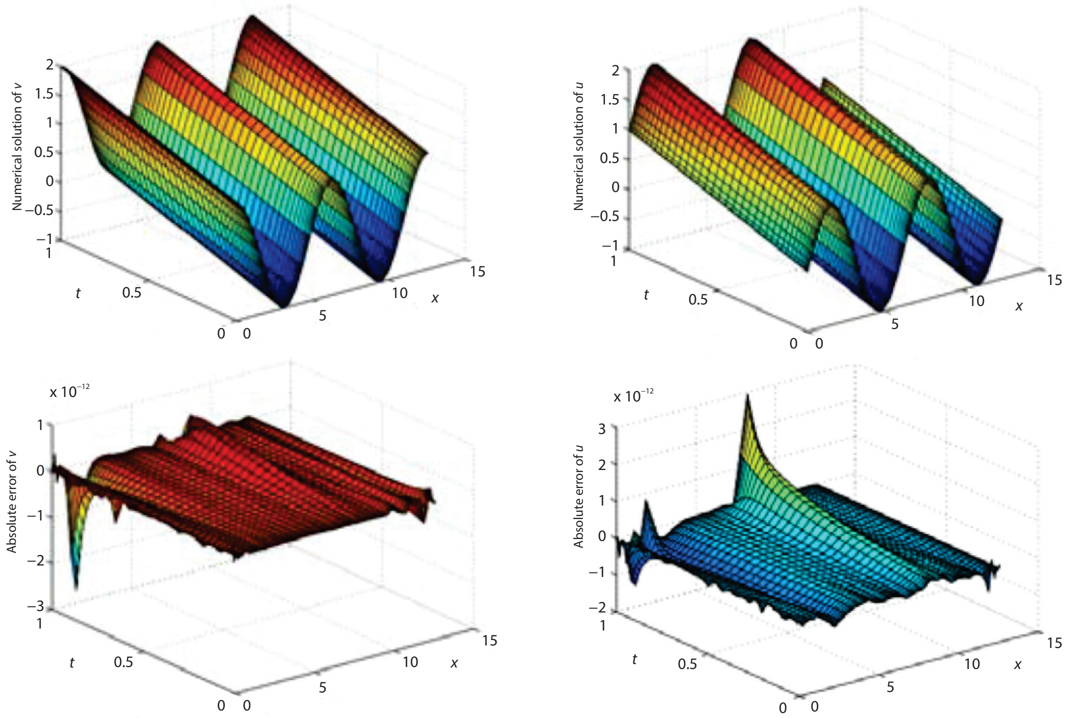

Figure 5. Numerical solutions and absolute errors for *Experiment 1* with M = 40, N = 40

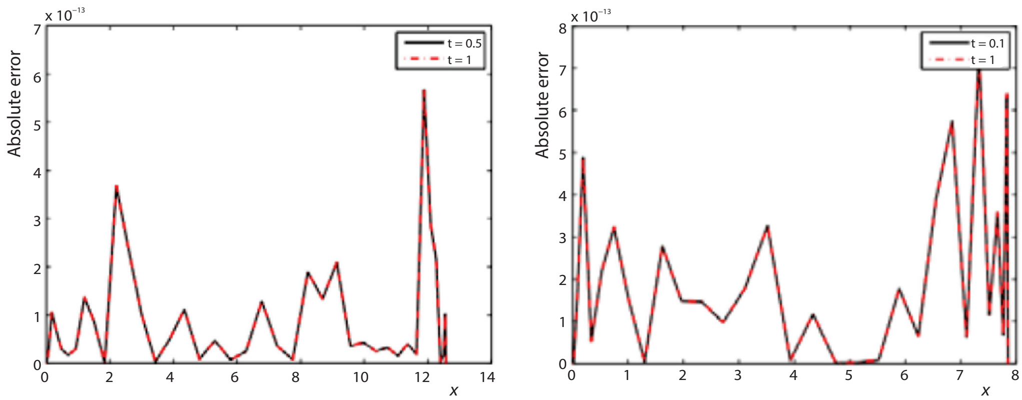

Figure 6. Comparison of absolute errors for *Experiment 1*

Table 2. Absolute errors for *Experiment 1* with M = 20, N = 20

$u(x, t)$	Numerical solution v	Exact solution v	Absolute error	Numerical solution u	Exact solution u	Absolute error
(0.35, 0.002)	0.0062	0.0062	0.0035e-10	0.4218	0.4218	0.0024e-9
(0.27, 0.003)	0.0245	0.0245	0.0215e-10	0.5000	0.5000	0.0114e-9
(1.32, 0.012)	0.0545	0.0545	0.0310e-10	0.5782	0.5782	0.1023e-9
(2.78, 0.034)	0.0955	0.0955	0.0445e-10	0.6545	0.6545	0.1425e-9
(3.24, 0.523)	0.1464	0.1464	0.1021e-10	0.7270	0.7270	0.1573e-9
(5.48, 0.598)	0.2061	0.2061	0.2017e-10	0.7939	0.7939	0.2347e-9

Table 3. Absolute errors for *Experiment 1* with M = 40, N = 40

$u(x, t)$	Numerical solution v	Exact solution v	Absolute error	Numerical solution u	Exact solution u	Absolute error
(3.18,0.001)	0.0015	0.0015	0.0023e-12	0.1753	0.1753	0.4201e-12
(2.97,0.014)	0.0062	0.0062	0.0134e-12	0.2061	0.2061	0.5137e-12
(6.23,0.028)	0.0138	0.0138	0.0223e-12	0.2388	0.2388	0.5328e-12
(7.59,0.049)	0.0245	0.0245	0.1543e-12	0.3087	0.3087	0.6217e-12
(8.90,0.301)	0.0381	0.0381	0.2321e-12	0.3455	0.3455	0.6357e-12
(8.95,0.312)	0.0737	0.0737	0.3861e-12	0.3833	0.3833	0.7211e-12

Experiment 2. *Experiment 1* is joined with the following initial conditions and Dirichlet boundary conditions:

$$u(x,0) = \sin x, \quad v(x,0) = \cos x, \quad x \in \left[0, \frac{5}{2}\pi\right]$$

$$u(0,t) = t, u\left(\frac{5}{2}\pi, t\right) = t+1, \quad v(0,t) = t+1, v\left(\frac{5}{2}\pi, t\right) = t, \quad t \in [0,1]$$

The exact solution is given by $u = t + \sin x$, $v = t + \cos x$. We take $d_1 = 0.5$, $d_2 = 0.1$, $a_1 = 0.5$, and $a_2 = 0.1$.

From the figs. 7 and 8 and tab. 4, it can be seen that when the number of nodes is increased, the absolute error tends to be stable and convergence rapidly, which indicates that the present method has good stability and convergence. It can be seen from *Experiments 1* and *2* that when spatial x selects different ranges, the influence of numerical solutions is small. With different spatial values, when the number of nodes is greater, the absolute error is smaller.

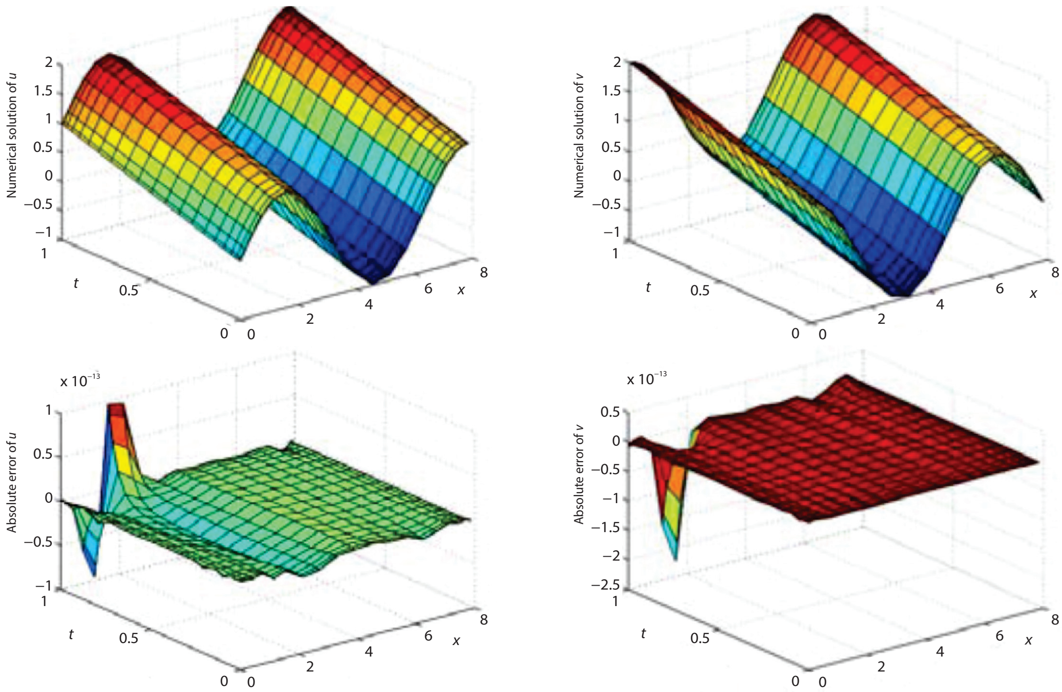

Figure 7. Numerical solutions and absolute errors for *Experiment 2* with M = 20, N = 20

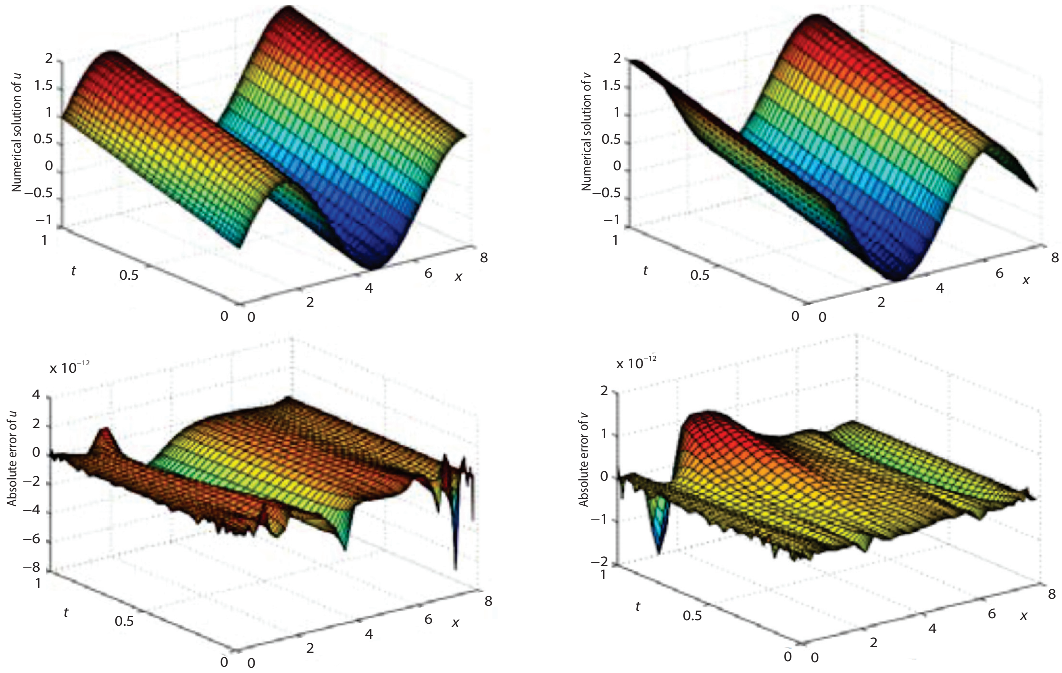

Figure 8. Numerical solutions and absolute errors for *Experiment 2* with $M = 40$, $N = 40$

Table 4. Absolute errors for *Experiment 2* with $M = 40$, $N = 40$

$u(x, t)$	Numerical solution v	Exact solution v	Absolute error	Numerical solution v	Exact solution u	Absolute error
(0.21,0.001)	1.0222	1.0222	0.0007e-12	0.7256	0.7256	0.1034e-12
(1.34,0.018)	1.0711	1.0711	0.1015e-12	0.9756	0.9756	0.1124e-12
(2.18,0.003)	1.1216	1.1216	0.2037e-12	1.4756	1.4756	0.2157e-12
(0.17,0.508)	1.1733	1.1733	1.3009e-12	1.5971	1.5971	0.3210e-12
(2.10,0.019)	1.2256	1.2256	1.3472e-12	1.6301	1.6301	0.3789e-12
(2.55,0.149)	1.2778	1.2778	2.0097e-12	1.7146	1.7146	0.4321e-12

Experiment 3. We consider the following system having time-dependent model parameters and a non-linear reaction term [14]:

$$\begin{cases} \dfrac{\partial u}{\partial t} = \dfrac{t}{2}\dfrac{\partial^2 u}{\partial x^2} - t\dfrac{\partial u}{\partial x} + (u-v)^2 + u^2 + v^2 - 2t^2 \\ \dfrac{\partial v}{\partial t} = \dfrac{t}{4}\dfrac{\partial^2 v}{\partial x^2} + \dfrac{t}{2}\dfrac{\partial v}{\partial x} + uv - t^2 - \dfrac{\sin(4x)}{2} + 1 \end{cases} \tag{13}$$

with the following initial and periodic boundary condition:

$$u(x,0) = -\sin 2x, \quad v(x,0) = -\cos 2x, \quad x \in [0, 4\pi]$$

$$u(0,t) = t = u(4\pi, t), \quad v(0,t) = t - 1 = v(4\pi, t) = t, \quad t \in [0,1]$$

The exact solution is $u = t - \sin 2x$, $v = t - \cos 2x$. The numerical solution and the absolute error diagram of *Experiment 3* are given in fig. 9, respectively. As can be seen from the fig. 9, the method can be used to obtain a smaller absolute error.

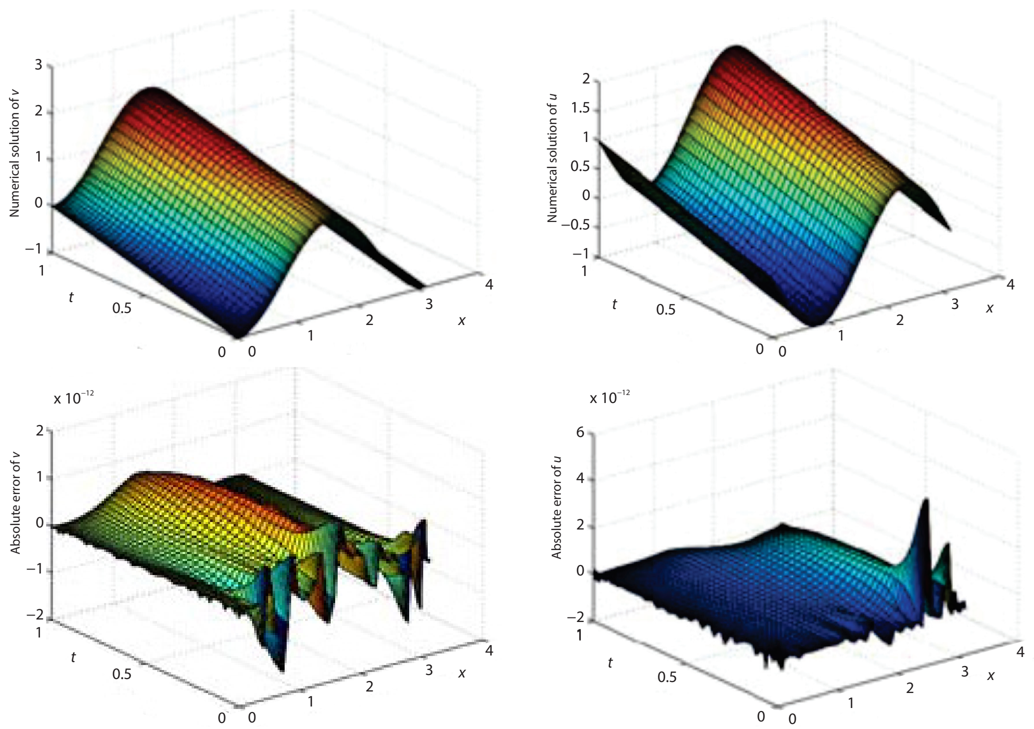

Figure 9. Numerical solutions and absolute errors for *Experiment 3* with M = 50, N = 50

Conclusion

In the present work, a class of advection-reaction-diffusion systems have solved by using barycentric interpolation collocation method. The numerical experiments show that the algorithm is high accuracy. We will apply this approach to more areas in the future.

Acknowledgment

The authors would like to express their thanks to the unknown referees for their careful reading and helpful comments. This paper is supported by Inner Mongolia Grassland Talent Project (No. 12000-12102012), Project of Inner Mongolia Institute of Data Science and Big Data (No. BDY18007), Inner Mongolia Medical University Excellent Teacher Project (NYJTXX201915).

References

[1] Tamsir, M., *et al.*, Numerical Computation of Non-Linear Fisher's Reaction-Diffusion Equation with Exponential Modified Cubic B-Spline Differential Quadrature Method, *International Journal of Applied and Computational Mathematics*, *4* (2018), 3, pp. 1-6
[2] Dhiman, N., Tamsir, M., A Collocation Technique Based on Modified Form of Trigonometric Cubic B-Spline Basis Functions for Fishers Reaction-Diffusion Equation, *Multidiscipline Modelling in Materials and Structures*, *14* (2018), 5, pp. 923- 939
[3] He, J. H., Approximate Solution of Non-Linear Differential Equations with Convolution Product Non-Linearities, *Computer Methods in Applied Mechanics and Engineering*, *167* (1998), 1-2, pp. 69-73
[4] He, J. H., Homotopy Perturbation Method: A New Non-linear Analytical Technique, *Applied Mathematics Computation*, *135* (2003), 1, pp. 73-79

[5] Yang, X. J., A New Integral Transform Operator for Solving the Heat-diffusion Problem, *Applied Mathematics Letters*, *64* (2017), Jan., pp. 193-197
[6] Ambrosio, D., *et al*., Adapted Numerical Methods for Advection-Reaction-Diffusion Problems Generating Periodic Wavefronts, *Computers and Mathematics with Applications*, *74* (2017), 5, pp. 1029-1042
[7] Jiwari, R., *et al*., Numerical Simulation Capture the Pattern Formation of Coupled Reaction-Diffusion Models, *Chaos, Solitons and Fractals*, *103* (2017), 5, pp. 422-439
[8] Li, S. P., *et al*., *Barycentric Interpolation Collocation Method for Non-Linear Problems*, National Defense Industry Press, Beijing, China, 2015
[9] Li, S. P., *et al*., High-Precision Non-Grid Center of Gravity Interpolation Collocation Method: Algorithm, *Program and Engineering Application*, Science Press, Beijing, China, 2012
[10] Zhou X. F., *et al*., Numerical Simulation of a Class of Hyperchaotic System Using Barycentric Lagrange Interpolation Collocation Method, *Complexity*, *2019* (2019), ID 1739785
[11] Liu, F. F., *et al*., Barycentric Interpolation Collocation Method for Solving the Coupled Viscous Burgers' Equations, *International Journal of Computer Mathematics*, *95* (2018), 11, pp. 2162-2173
[12] Wu, H. C., *et al*., Numerical Solution of a Class of Non-Linear Partial Differential Equations by Using Barycentric Interpolation Collocation Method, *Mathematical Problems in Engineering*, *2018* (2018), ID 7260346
[13] Du, M. J., Li, J. M., *et al*., Numerical Simulation of a Class of 3-D Kolmogorov Model with Chaotic Dynamic Behavior by Using Barycentric Interpolation Collocation Method, *Complexity*, *2019* (2019), ID 3426974
[14] D'Ambrosio, R., *et al*., Adapted Numerical Methods for Advection-Reaction-Diffusion Problems Generating Periodic Wavefronts, *Computers and Mathematics with Applications*, *74* (2017), 5, pp. 1029-1042

Paper submitted: August 3, 2018
Paper revised: November 29, 2018
Paper accepted: February 21, 2019